Journal of
Nanoscience and Nanotechnology
Vol. 7, 1–8, 2007

Mechanical Behaviors of Carbon Nanotubes with Randomly Located Vacancy Defects

Wenyi Hou[1] and Shaoping Xiao[2,*]

[1] *Department of Mechanical and Industrial Engineering and Center for Computer-Aided Design, The University of Iowa, Iowa City, IA 52242, USA*
[2] *3131 Seamans Center, The University of Iowa, Iowa City, IA 52241, USA*

In this paper, (10, 0) zigzag nanotubes and (6, 6) armchair nanotubes are considered to investigate the effects of randomly distributed vacancy defects on mechanical behaviors of single-walled carbon nanotubes. A spatial Poisson point process is employed to randomly locate vacancy defects on nanotubes. Atomistic simulations indicate that the presence of vacancy defects result in reducing nanotube strength but improving nanotube bending stiffness. In addition, the studies of nanotube torsion indicate that vacancy defects prevent nanotubes from being utilized as torsion springs.

Keywords: Carbon Nanotubes, Mechanical Properties, Vacancy Defects.

RESEARCH ARTICLE

1. INTRODUCTION

The discovery of carbon nanotubes (CNTs) in 1991 (Ref. [1]) has inspired researchers to intensively study the mechanics of CNTs and their applications in nanoscale materials and devices due to their unique mechanical, electrical, and thermal properties. Theoretical analysis[2] indicated that single-walled carbon nanotubes (SWNTs) could possess extremely high tensile strengths (~300 GPa), while failure strains have been predicted to be as high as ~30%. However, based on experiments of nanotube fracture reported by Yu et al.,[3] the observed failure stresses ranged from 11 to 63 GPa, while failure strains ranged from 2 to 13%. Other experiments and numerical analyses[4–10] also showed significant variation in mechanical properties of nanotubes. A survey[11] on the statistical properties of the elastic moduli and strengths of CNTs illustrated that the Young's moduli of CNTs were found to range from 0.1 to 1.6 Tpa, and the strengths varied from 5 to 150 Gpa. Such variations might be due to the heterogeneity of CNTs, the size of tested samples, temperatures, defects, or systematic errors in measurements. The above uncertainties should be considered when investigating the mechanical behaviors of CNTs and their applications in nanoscale materials and devices.

Researchers have studied the effects of some uncertainties mentioned above on the mechanics of nanotubes. Zhao et al.[5] predicted that the nanotube strength depended on the nanotube structure, including chirality and diameter, and other factors such as temperature and strain rate. The effects of size and chirality on nanotubes' mechanical properties have also been studied.[6–8] Some researchers who attempted to resolve the theoretical-experimental discrepancies have concentrated on the possible role of defects in decreasing strengths of CNTs. It has been shown that defects played a significant role in the mechanics of nanotubes, especially nanotube fracture.[9] Defects in nanotubes, including vacancies, metastable atoms, pentagons, heptagons, heterogeneous atoms, discontinuities of walls, distortion in the pacing configuration of and CNT bundles, were widely observed in CNTs.[12,13] Among those types of defects, the Stone-Wales (SW) defects[10,11] have received the most consideration. Yakobson[2] proposed that aggregations of SW defects could be followed by a ring-opening mechanism that would permit the nucleation of a crack. However, quantum mechanics calculations[14] have illustrated that SW defects—even multiple adjacent and pre-existing ones—did not markedly reduce the failure stresses and strains of CNTs. It should be noted that Lu and Bhattacharya[11] employed a spatial Poisson point process and a Matern hard-core random field on a finite cylindrical surface to describe the random distribution of the SW defects. They numerically demonstrated that the random SW defects had pronounced effects on mechanical properties.

Vacancy defects, i.e., defects resulting from missing carbon atoms, are likely candidates to severely reduce the strength of CNTs. Such defects could be caused by ion

*Author to whom correspondence should be addressed.

irradiation, absorption of electrons, or CNT fabrication processes. The vacancy defects have received considerable attention. Mielke et al.[9] employed molecular mechanics and quantum mechanics calculations to explore the role of vacancy defects in the fracture of CNTs under uniaxial tension. They concluded that one- and two-atom vacancy defects could reduce failure stresses of CNTs by up to 26%. Xiao and Hou[15] studied the fracture of vacancy-defected nanotubes and their embedded nanocomposites. They also pointed out that vacancy defects could dramatically reduce the failure stresses and strains of CNTs and nanotube-embedded composites. In addition, they found that nanocomposites in which vacancy-defected nanotubes were embedded exhibited different characteristics than those in which pristine nanotubes were embedded.

In the above studies, only a single vacancy defect was considered and located in the middle of CNTs. However, the number, location, and type of vacancy defects are not deterministic variables, and their randomness is induced by CNT growth procedures, the oxidative purification process, or surrounding temperatures. In this paper, we first classified the vacancy defects into three basic types: one-atom vacancy defects, two-atom vacancy defects, and cluster-atom vacancy defects. We also adapted the spatial Poisson point process to randomize vacancy defects. The process differs from that described by Lu and Bhattacharya[11] in that the cutoff distance is not employed so that various types of vacancy defects can be randomized. Then, we investigate the effects of randomly located vacancy effects on mechanical behaviors of CNTs, including nanotube fracture, bending, and torsion.

2. ATOMISTIC METHOD AND THE POTENTIAL FUNCTION

We use molecular mechanics calculation, also known as the force field calculation, to determine the equilibrium configurations of the simulated nanotubes via the minimization of the nanotube potential. Without the consideration of external forces, the governing equations in molecular mechanics calculations are expressed as:

$$\frac{\partial E(\mathbf{x})}{\partial \mathbf{x}_I} = 0 \tag{1}$$

where $\mathbf{x}_I$ is the location of atom I and E is the potential energy. In this paper, we employ the modified Morse potential function, proposed by Belytschko et al.,[16] to describe the interaction between bonded carbon atoms. The modified Morse potential function is written as

$$\begin{aligned} E &= E_{\text{stretch}} + E_{\text{angle}} \\ E_{\text{stretch}} &= D_e\{[1-e^{-\beta(r-r_0)}]^2 - 1\} \\ E_{\text{angle}} &= \frac{1}{2}k_\theta(\theta-\theta_0)^2[1+k_s(\theta-\theta_0)^4] \end{aligned} \tag{2}$$

where E_{stretch} is the bond energy due to bond stretching or compressing, E_{angle} is the bond energy due to bond angle-bending, r is the current bond length, and θ is the angle of two adjacent bonds representing a standard deformation measure in molecular mechanics. The parameters are:

$$\begin{aligned} &r_0 = 1.42\times10^{-10}\ \text{m}, \quad D_e = 6.03105\times10^{-19}\ \text{Nm} \\ &\beta = 2.625\times10^{10}\ \text{m}^{-1}, \quad \theta_0 = 2.094\ \text{rad} \\ &k_\theta = 1.13\times10^{-18}\ \text{Nm/rad}^2, \quad k_s = 0.754\ \text{rad}^{-4} \end{aligned} \tag{3}$$

It has been shown that this potential function results in reasonable Young's modulus and Poisson's ratio of nanotubes compared with experimental investigations. Belytschko and his co-workers[16] also showed that the modified Morse potential could predict nanotube fracture better than the Brenner's potential.[17]

3. VACANCY DEFECTS

3.1. One-Atom Vacancy Defect

If a single carbon atom marked with a circle as shown in Figure 1(a) is removed from the lattice, its three neighbors, n_1, n_2, and n_3, will become less stable because their sp2 bonds are not saturated. Any two of these carbon atoms can be reconnected to form a new bond. Consequently, a five-member and a nine-member ring are reconstructed.[9] For both armchair and zigzag CNTs, the reconstruction results in one symmetric configuration and two asymmetric configurations as shown in Figures 1(b–d). We think that the above three configurations have the same probability of appearing during the bond reconstruction process because each of them results in a similar potential. It should be noted that the distances between any two unsaturated atoms are identical (= 0.2469 nm) without considering the curvature effects of CNTs.

3.2. Two-Atom Vacancy Defect

A two-atom vacancy defect is modeled by taking out two adjacent carbon atoms followed by bond reconstruction, as shown in Figure 2. When the two adjacent carbon atoms i and j, forming one C=C sp2 bond, are taken out, the four neighboring atoms become unsaturated. Although there are several possible configurations during the bond reconstruction processes, we only consider the one shown in Figure 2(b) because the distances between n_1 and n_2 and between n_3 and n_4 are the smallest compared to the distances of any other combinations. Consequently, the configuration in Figure 2(b) results in the minimal potential. Hence, two five-member rings and one eight-member ring exist. It should be noted that such a configuration could be asymmetric if two atoms that form a bond not parallel to the tube axis were taken out.

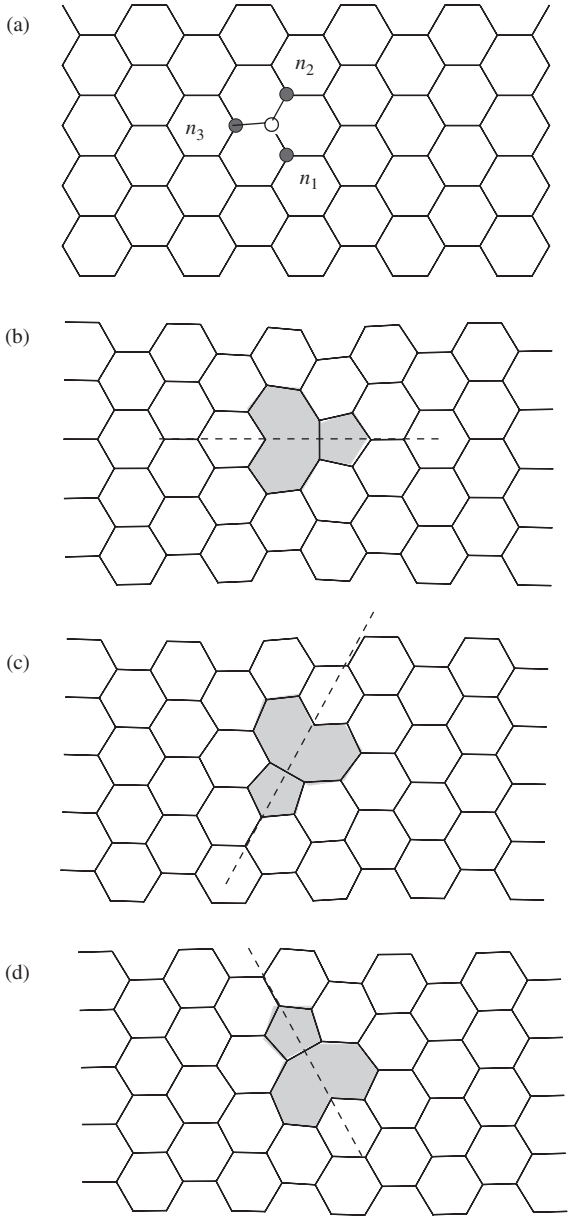

Fig. 1. One-atom vacancy defects: (a) a single atom is selected to be taken out; (b) atoms n_1 and n_2 are connected; (c) atoms n_1 and n_3 are connected; (d) atoms n_2 and n_3 are connected.

3.3. Cluster-Atom Vacancy Defect

A cluster-atom vacancy defect is created if more than two carbon atoms are taken out at one location, generating a hole[9] or a crack.[15] Since the number of missing atoms is larger than two, there are many possible configurations during the bond reconstruction. In this paper, we only consider connecting the two unsaturated atoms that are neighbors of the same missing atom. The distance between those two unsaturated atoms must be the least distance between any two unsaturated carbon atoms, and the resulting potential is minimal. Figure 3 shows one example of cluster-atom vacancy defects.

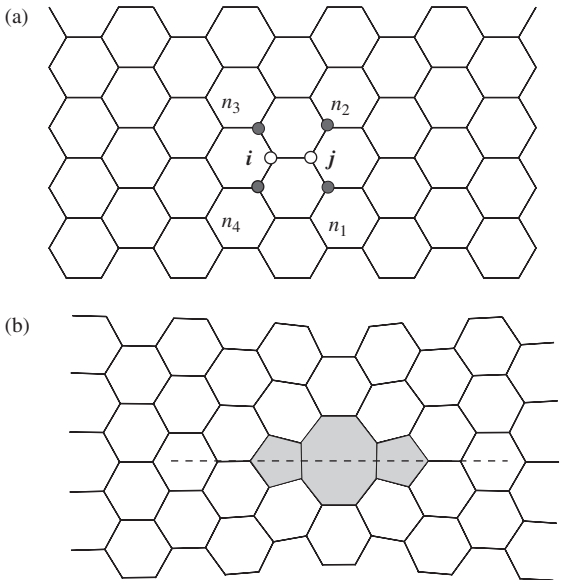

Fig. 2. A two-atom vacancy defect.

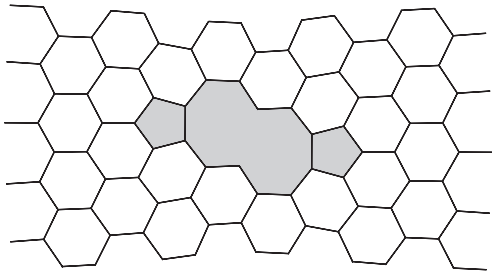

Fig. 3. A cluster-atom vacancy defect.

4. RANDOMIZATION OF VACANCY DEFECTS

Obviously, a three-dimensional (3D) random field model is needed to describe the uncertainties of vacancy defects on nanotubes. However, due to the unique structures of SWNTs, they can be mapped onto two-dimensional (2D) graphene planes with a thickness of 0.34 nm. Therefore, a 3D model can be simplified as a 2D surface problem. Two primary uncertainties of vacancy defects are considered in this paper: (1) the number of missing atoms and (2) the location of a vacancy defect.

4.1. Poisson Point Process

Since vacancy defects occur on CNTs in a completely random manner, a homogeneous Poisson point process is employed to determine the number of Poisson points, i.e., the number of missing atoms, in this paper. The probability of the number (k) of Poisson points occurring in a finite 2D plane can be expressed by:

$$P(N(A) = k) = \frac{e^{-\lambda A}(\lambda A)^k}{k!}, \quad k = 1, 2, 3, \ldots \qquad (4)$$

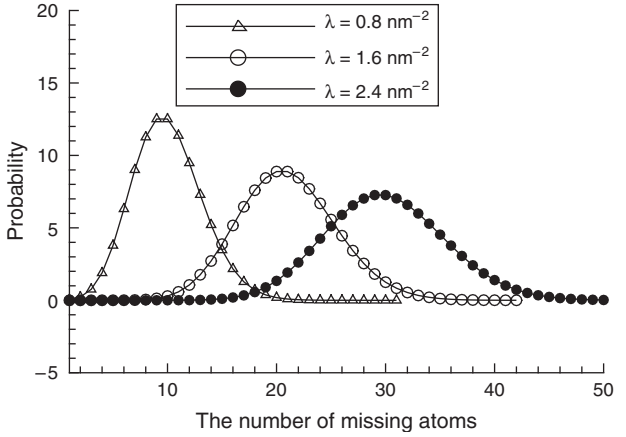

Fig. 4. Probability distribution of the number of missing atoms.

where A is the plane area, $N(A)$ is the number of Poisson points on this area A, and λ is the Poisson point density per area. $N(A)$ and λ are also called the number of missing atoms and the missing atom density, respectively, in this paper. It is clear that different missing atom densities will result in different probability distributions of the number of missing atoms. Here, we treat λ as an independent variable and limit its value to between 0 and 2.5 nm^{-2}. In this paper, we mainly consider (10, 0) zigzag nanotubes and (6, 6) armchair nanotubes, which have similar length (5 nm) and diameter (0.8 nm). Consequently, their surface areas are around $A = 12$ nm^2. Figure 4 illustrates the probability distributions of the number of missing atoms at various missing atom densities.

Here, we take the missing atom density of 0.8/nm^2 as an example. The numbers of missing atoms are in the range of 0 to 20, and each number of missing atoms has its own probability of occurrence, as shown in Figure 4. For instance, the occurrence probability of 12 missing atoms is about 9%. If one hundred computational samples are chosen to study the statistical properties of the mechanical behavior of vacancy-defected nanotubes with $\lambda = 0.8$ nm^{-2}, there must be nine samples containing 12 missing atoms. It should be noted that Eq. (4) is only utilized to determine the occurrence probability of missing atoms.

4.2. Randomize Locations of Vacancy Defects

To randomize the locations of vacancy defects, we first assume that the Poisson points are uniformly distributed in a 2D plane, to which the surface of a nanotube can be mapped. The atom that is the closest to a Poisson point is indicated as the missing atom. After the missing atoms are located, a defect site is denoted as the location containing one or several missing atoms neighboring each other. The number of missing atoms in a defect site results in the type of generated vacancy defect after taking out the missing atoms and reconstructing bonds. As mentioned above, the one-atom vacancy defect has three possible configurations that have the same probability of occurrence. Therefore, randomly choosing one of those three configurations is involved in the generation of one-atom vacancy defects. It should be noted that Lu and Bhattacharya[11] also used a similar procedure to generate the Stone-Wales defects. However, they introduced the Matern hard-core process involving cutoff distances for each Poisson point to avoid the overlapping of defects. In our paper, we do not need to prevent the neighboring missing atoms because it is possible to generate a large vacancy defect if a defect site contains more than one missing atom.

As an example, Figure 5 illustrates the generation of vacancy defects on a (10, 0) nanotube with 12 missing atoms. First, 12 Poisson points are deposed onto a 2D plane on which the surface of the considered (10, 0) nanotube is mapped. The coordinates of each Poisson point are randomly selected within this 2D plane as shown in Figure 5(a). Then, the carbon atoms that are closest to each Poisson point are marked with circles as missing atoms, as shown in Figure 5(b). If more than one atom has an identical least distance to one Poisson point, the missing atom is randomly selected. Finally, bond reconstructions are

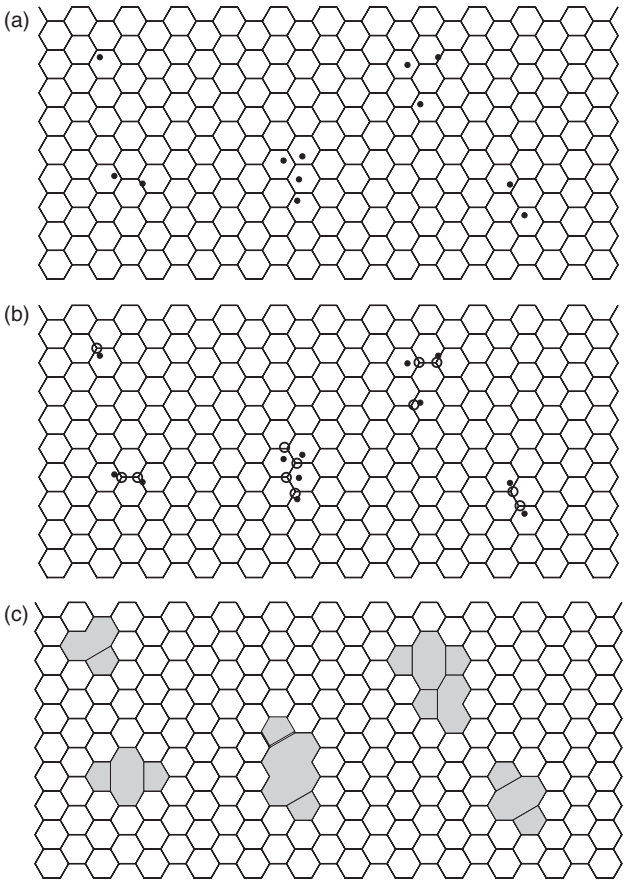

Fig. 5. Generation of vacancy defects on a grapheme sheet. (a) Poisson points are deposed on a two-dimensional plane on which a (10, 0) nanotube is mapped; (b) search and mark the missing atoms with circles; (c) bond reconstruction for vacancy defects.

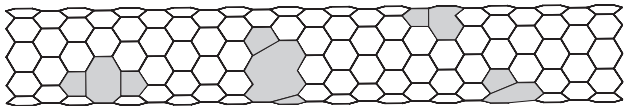

Fig. 6. Configuration of a (10, 0) nanotube containing randomly located vacancy defects illustrated in Figure 5.

processed according to the location of the missing atoms to generate corresponding vacancy defects as described earlier. Figure 5(c) shows that this sample contains two one-atom vacancy defects, three two-atom vacancy defects, and one cluster-atom vacancy defect. The configuration of the corresponding (10, 0) zigzag nanotube is shown in Figure 6. It is obvious that the numbers of vacancy defects vary from case to case even if the numbers of missing atoms are the same.

For convenience, we assume that each atom occupies the same volume. Consequently, the volume fraction of vacancy defects is calculated as the ratio of the number of missing atoms to the number of total atoms in the pristine nanotube. In other words, the average volume fraction of vacancy defects, V_{frac}, is determined by the average number of missing atoms, which is $N_{\text{avgMiss}} = \lambda A$.

5. MECHANICAL BEHAVIORS OF VACANCY-DEFECTED NANOTUBES

5.1. Nanotube Fracture

Several researchers[9, 15] have studied the fracture of vacancy-defected nanotubes. However, the main focuses of the investigations were nanotubes containing one vacancy defect located in the middle of the nanotube. In this section, we will study the effects of randomly located vacancy defects on nanotube fracture. (10, 0) Zigzag nanotubes and (6, 6) armchair nanotubes are considered here. Size effects are ignored based on previous research.[6]

To perform the simulation, we first randomly deploy vacancy defects on nanotubes, based on the procedure described in Section 4. One end of the nanotube is fixed and the other is gradually elongated with the prescribed displacement. The conjugate gradient method is used to minimize the system potential energy during the molecular mechanics calculation at each displacement increment. The applied external force F is calculated by summing the internal forces of atoms on the prescribed end. One can compute the stress via $\sigma = F/(\pi Dh)$ where D is the tube diameter and h is the tube thickness of 0.34 nm. Details about the atomistic simulation of nanotube fracture are provided by Belytschko et al.[16]

The histogram in Figure 7 illustrates the frequencies of occurrence of failure stresses for (10, 0) zigzag nanotubes when the missing atom density is 1.6 nm^{-2}. In this case, the average number of missing atoms is 20, and the average volume fraction of vacancy defects is 4%. 100 simulations are conducted, and nanotube failure stress fits normal

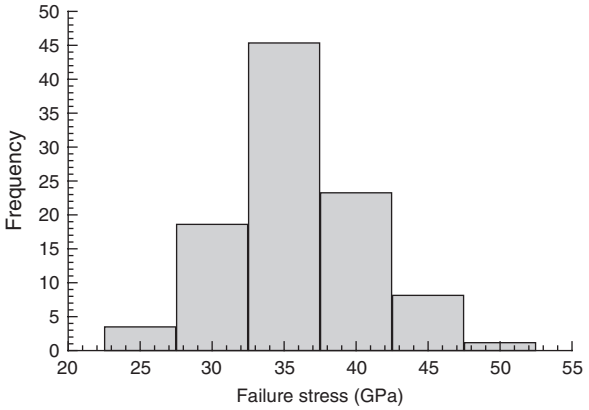

Fig. 7. Frequency of occurrences of nanotube failure stresses when $\lambda = 1.6$ nm^{-2}.

distribution as shown in Figure 7. The calculated mean value of failure stress is 38.3 GPa, and the standard deviation is 4.50 GPa.

The relationship between the failure stress and the missing atom density is illustrated in Figure 8 for both (10, 0) nanotubes and (6, 6) nanotubes. Since the missing atom density determines the average volume fraction of vacancy defects, Figure 8 also indicates the effect of volume fraction of vacancy defects on nanotube fracture. It has been predicted that pristine zigzag nanotubes have a failure stress of 90 GPa while pristine armchair nanotubes have a failure stress of 110 GPa.[16] Figure 8 shows that even a small average volume fraction of 0.2% (the missing atom density is 0.08 nm^{-2}) can dramatically reduce nanotube failure stresses: the average failure stresses are 60 GPa and 70 GPa for zigzag nanotubes and armchair nanotubes, respectively. From Figure 8 we also can see that larger defect sizes result in lower failure stresses. When the average volume fraction of vacancy defects is increased to 5% (the missing atom density is 2.0 nm^{-2}), mean failure stresses of zigzag and armchair nanotubes are reduced to 36 GPa and 40 GPa, respectively.

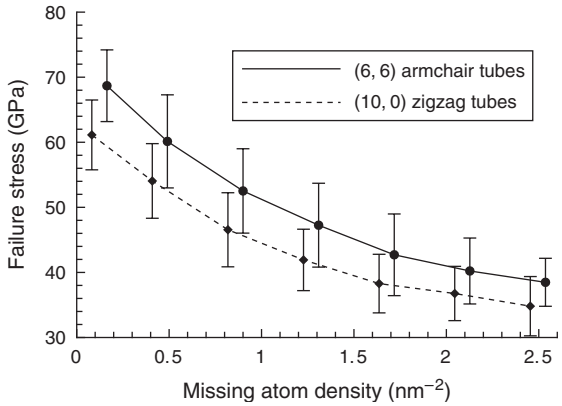

Fig. 8. Failure stresses of vacancy-defected nanotubes. (Solid and dashed lines represent mean values of failure stresses; vertical lines represent +/− one standard deviation).

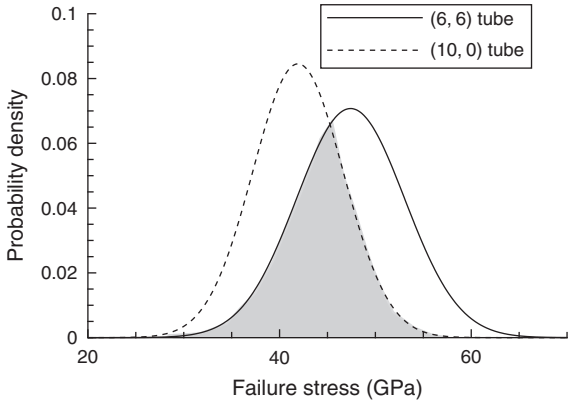

Fig. 9. Probability distributions of failure stresses.

Generally, armchair nanotubes have higher mean failure stresses than zigzag nanotubes, as shown in Figure 8. However, due to the uncertainties of vacancy defects, it is possible that zigzag nanotubes have higher failure stresses than armchair nanotubes at the same missing atom density. Figure 9 shows that the probability distributions of failure stresses of (10, 0) zigzag nanotubes and (6, 6) armchair nanotubes overlap each other when the missing atom density is 1.2 nm^{-2}, i.e., the average volume fraction of vacancy defects is 3%. In this case, the probability that (10, 0) zigzag tubes have higher failure stresses than (6, 6) armchair tubes is 59%, which is the area of the shaded region in Figure 9. Such a probability is larger in the case of a higher average volume fraction of vacancy defects, as illustrated in Figure 8.

5.2. Nanotube Bending

Nanotubes can be utilized in nano-device design due to their unique mechanical and electrical properties. Kim and Lieber[18] fabricated nanotweezers based on cantilevered CNTs. Voltages applied to the electrodes closed and opened the free ends for manipulation and interrogation of nanostructures. Dequesnes et al.[19] designed and simulated cantilevered CNTs over a graphite ground as nano-switches. It is evident that the bending stiffness of CNTs is key to these nano-devices. In this paper, we will investigate the effects of randomly located vacancy defects on bending of clamped–clamped CNTs, as shown in Figure 10.

To simplify the model due to its symmetry, we only model the left half of the clamped–clamped nanotubes using (6, 6) and (10, 0) nanotubes with the length of 5 nm. One end of the carbon is fixed, and the prescribed deflection is applied at another end. Then a conjugate gradient method is used to minimize the system potential energy for any given prescribed deflection. The procedures are repeated until a required deflection (Δx) is reached. The corresponding vertical force, P, is calculated by summing the internal forces of atoms at the prescribed boundary.

Figure 11 shows the relationship between the applied force and the missing atom density at various required

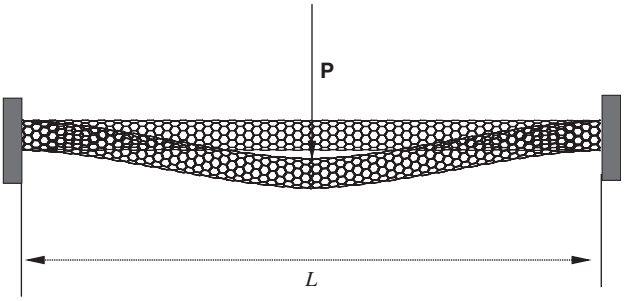

Fig. 10. Bending of a clamped–clamped nanotube.

deflections. (6, 6) Armchair nanotubes, on average, request larger forces than (10, 0) zigzag nanotubes to reach the same deflection if they have the same missing atom density. Since the bending stiffness is determined by the ratio of applied force to the deflection, we can conclude that the mean bending stiffness of armchair tubes is higher than that of zigzag nanotubes. Such a conclusion was also obtained for pristine tubes using the elastic shell theory.[20] In addition, Figure 11 shows that the mean applied force increases with the increasing missing atom density for any required deflection. For example, when the missing atom density is 1.6 nm^{-2}, i.e., the mean volume fraction of vacancy defects is 4%, a mean force of 3.3 nN is required to reach the deflection of 0.275 nm on (6, 6) armchair tubes. However, the pristine tube needs only 2.4 nN to reach the same deflection. In other words, vacancy defects can enhance the bending stiffness of clamped–clamped nanotubes. On average, a larger volume fraction of vacancy defects results in higher bending stiffness. We think this phenomenon is due to residual stresses that are generated along the clamped–clamped CNTs because of the vacancy defects at the initial configurations. Figure 11 also shows that vacancy defects have more significant effects on the bending stiffness of armchair nanotubes than

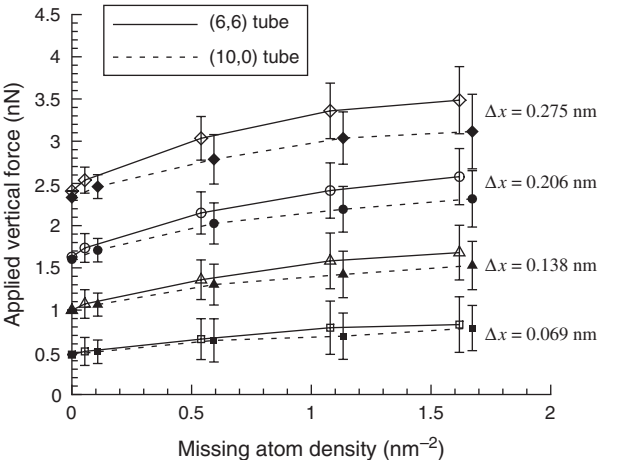

Fig. 11. The corresponding forces applied on vacancy-defected nanotubes to reach required deflections. (Solid and dashed lines represent mean values of applied forces; vertical lines represent +/− one standard deviation).

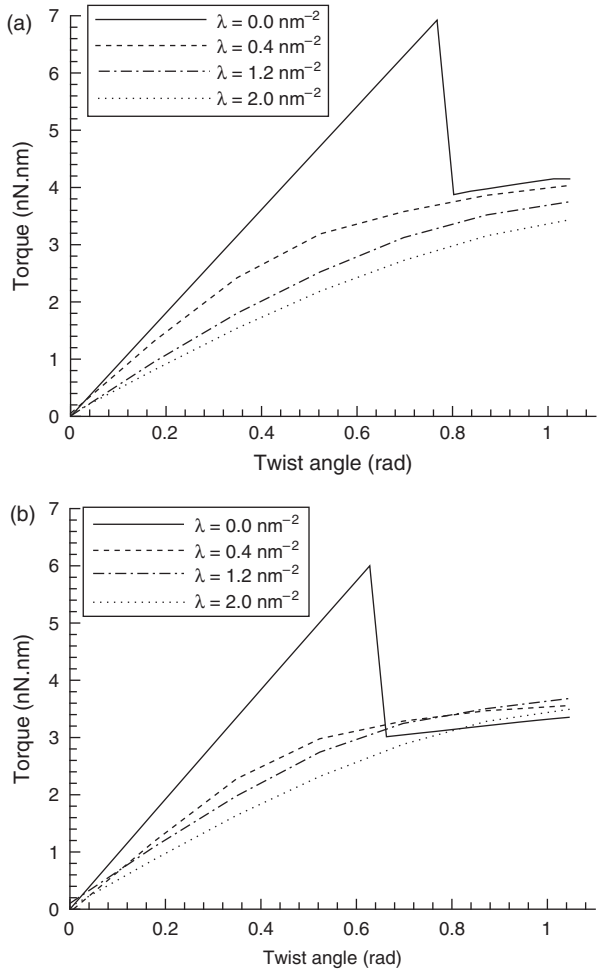

Fig. 12. The relationship between mean torques and angles of twist for (a) (10, 0) zigzag nanotubes and (b) (6, 6) armchair nanotubes.

zigzag nanotubes when nanotubes are subject to a larger deflection. It should be noted that we did not consider nanotube failure due to bending.

5.3. Nanotube Torsion

Carbon nanotubes can also be used as torsion springs and mechanical supports for the nano-devices. Meyer and his co-workers[21] built a torsional pendulum based on an individual single-walled carbon nanotube. Papadakis et al.[22] fabricated the resonant oscillators using multi-walled CNTs. In this paper, we also investigate the vacancy effects on mechanical behaviors of nanotube-based torsion springs. (6, 6) Armchair tubes and (10, 0) zigzag tubes that have similar sizes are still considered as they were before. During the molecular mechanics calculation, we fix one end of the nanotube and apply a prescribed angle of twist on the other end. The prescribed angle of twist is increased gradually, and the corresponding torque, **T**, is then computed as follows:

$$\mathbf{T} = \left(\sum_i \mathbf{r}_i \times \mathbf{F}_i\right)_z = \sum_i F_{yi} r_{xi} - F_{xi} r_{yi} \tag{5}$$

where $\mathbf{r}_i$ and $\mathbf{F}_i$ are the coordinate and the internal force of atom i, respectively. We assume that the z-axis follows the axial direction of the tube and passes its centroid.

Figure 12 shows the relationship between the angles of twist and the corresponding mean torque. The curve slope represents the torsional spring rate. We can see that the pristine (10, 0) tubes and (6, 6) tubes have a similar torsional spring rate of 9.0×10^{-16} Nm/rad. However, the critical angles of twist for nanotube buckling are different.

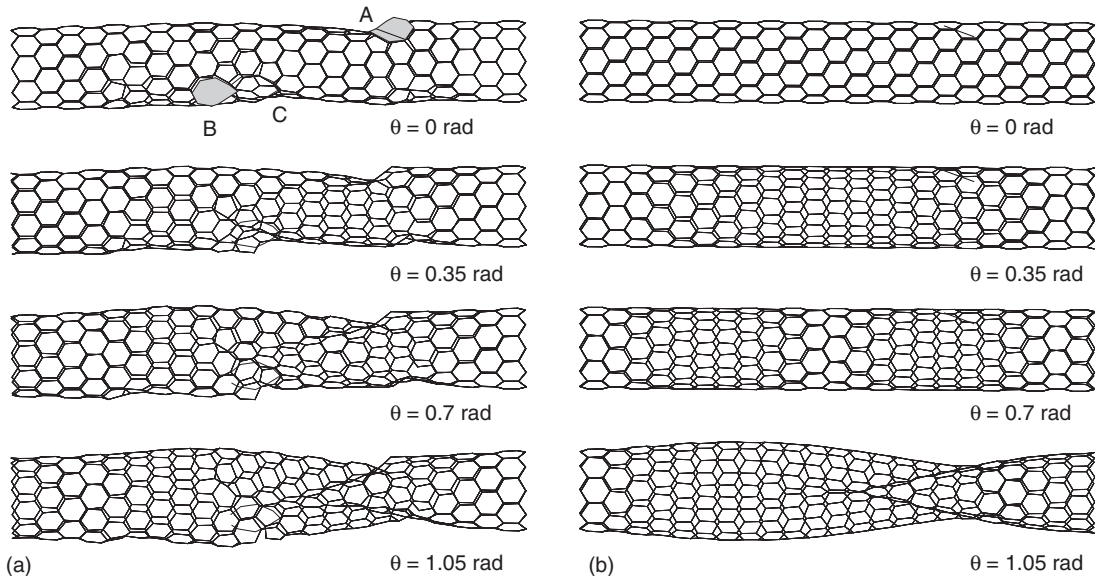

Fig. 13. The evolutions of the configuration of (a) a vacancy-defected (10, 0) nanotube and (b) a pristine (10, 0) nanotube.

Figure 12 shows that buckling occurs on the (10, 0) pristine zigzag tube when the angle of twist is 0.78 radian. The buckling on the (6, 6) armchair tube can be observed when the angle of twist is 0.6 radian.

Figure 12 also illustrates the comparison between vacancy-defected nanotubes and pristine tubes. The mean torque for vacancy-defected nanotubes is calculated based on 100 samples for any given missing atom density. We can clearly see that the torsional spring rates of nanotubes are severely reduced with the presence of vacancy defects for both zigzag and armchair tubes. The mean torsional spring rates of vacancy-defected nanotubes are 6.5×10^{-16}, 5×10^{-16}, and 4.5×10^{-16} Nm/rad when the missing atom densities are 0.4, 1.2, and 2.0 nm^{-2}, respectively. Such spring rates are valid when the angles of twist are smaller than 0.4 radian. Otherwise, the spring rates gradually decrease and can no longer sustain torsion. It is concluded that vacancy-defected nanotubes are not good candidates for torsional springs. In addition, no buckling is observed for vacancy-defected tubes.

Figure 13 compares the evolution of the configuration of a vacancy-defected (10, 0) nanotube with a pristine (10, 0) nanotube when the nanotubes are subject to torque. The defected tube in Figure 13(a) is one of the samples when the missing atom density is 0.8 nm^{-2}. Three vacancy defects can be observed, indicated by A, B, and C in the initial configuration. We see that local distortions occur at defect sites on the nanotube even with a small angle of twist. Such distortions become severe when the angle of twist increases, and the tube loses the capability to sustain torsion. However, the pristine (10, 0) tube can keep the cylindrical configuration under torsion until the occurrence of buckling, as illustrated in Figure 13(b).

6. CONCLUSIONS

In this paper, we use atomistic simulation to investigate the effects of randomly located vacancy defects on the mechanical behaviors of single-walled carbon nanotubes, including their fracture, bending, and torsion. Three types of vacancy defects are classified, and a spatial Poisson point process is employed to randomize the vacancy defects. Statistical properties of nanotube failure stress and bending stiffness are studied, based on 100 sample simulations of both nanotube fracture and clamped–clamped nanotube bending. We find that the vacancy defects can dramatically reduce nanotube strength but improve the bending stiffness. With the same mean volume fraction of vacancy defects, the zigzag nanotubes have lower mean failure stress and bending stiffness than the armchair nanotubes of similar size. However, due to the uncertainties of vacancy defects, it is possible that zigzag nanotubes have higher strength and bending stiffness than armchair nanotubes. In addition, the studies of nanotube torsions show that the vacancy-defected nanotubes cannot sustain large torque due to local severe distortions at defect sites. Consequently, nanotubes with vacancy defects are not suitable for use as torsion springs.

Acknowledgment: This research was supported by startup fund support from the College of Engineering and the Center for Computer-Aided Design (CCAD) at The University of Iowa, and by NSF under Grant No. 0630153.

References and Notes

1. S. Iijima, *Nature* 354, 56 **(1991)**.
2. B. I. Yakobson, *Appl. Phys. Lett.* 72, 918 **(1998)**.
3. M. F. Yu, O. Lourie, M. J. Dyer, K. Moloni, T. F. Kelly, and R. S. Ruoff, *Science* 287, 637 **(2000)**.
4. S. Xie, W. Li, Z. Pan, B. Chang, and L. Sun, *J. Phys. Chem. Solids* 61, 1153 **(2000)**.
5. Q. Z. Zhao, M. B. Nardelli, and J. Bernholc, *Phys. Rev. B* 65, 144105 **(2002)**.
6. S. P. Xiao and W. Y. Hou, *Fullerenes, Nanotubes, and Carbon Nanostructures* 14, 9 **(2006)**.
7. E. W. Wong, P. E. Sheehan, and C. M. Lieber, *Science* 277, 1971 **(1997)**.
8. E. Hernandez, C. Goze, P. Bernier, and A. Rubio, *Phys. Rev. Lett.* 80, 4502 **(1998)**.
9. S. L. Mielke, D. Troya, S. Zhang, J. Li, S. Xiao, R. Car, R. S. Ruoff, G. C. Schatz, and T. Belytschko, *Chem. Phys. Lett.* 390, 413 **(2004)**.
10. N. Chandra, S. Namilae, and C. Shet, *Phys. Rev. B* 69, 09101 **(2004)**.
11. Q. Lu and B. Bhattacharya, *Nanotechnology* 16, 555 **(2005)**.
12. F. Banhart, *Reports on Progress in Physics* 62, 1181 **(1999)**.
13. S. Iijima, T. Ichihashi, and Y. Ando, *Nature* 356, 1744 **(1992)**.
14. D. Troya, S. L. Mielke, and G. C. Schatz, *Chem. Phys. Lett.* 382, 133 **(2003)**.
15. S. Xiao and W. Hou, *Phys. Rev. B* 73, 115406 **(2006)**.
16. T. Belytschko, S. Xiao, G. C. Schatz, and R. Ruoff, *Phys. Rev. B* 65, 235430 **(2002)**.
17. D. W. Brenner, *Phys. Rev. B* 42, 9458 **(1990)**.
18. P. Kim and C. M. Lieber, *Science* 286, 2148 **(1999)**.
19. M. Dequesnes, S. V. Rotkin, and N. R. Aluru, *Nanotechnology* 2, 383 **(2002)**.
20. C. Q. Ru, *Phys. Rev. B* 62, 9973 **(2000)**.
21. J. C. Meyer, M. Paillet, and S. Roth, *Science* 309, 1539 **(2005)**.
22. S. J. Papadakis, A. R. Hall, P. A. Williams, L. Vicci, M. R. Falvo, R. Superfine, and S. Washburn, *Phys. Rev. Lett.* 93, 146101 **(2004)**.

Received: 11 July 2006. Revised/Accepted: 27 March 2007.